very smaller than the value of $\bar{f_l}$. This means that a gradual change of the steady state from one dominated by X^{ol} concentration at u_l^l to one of X^{oh} concentration at u_t^h will be observed. There is a discontinuous change from X^{ol} Gaussian to X^{oh} Gaussian at that value of $u = u_m$ satisfying Maxwell-type construction ($\bar{f_l}/\bar{f_h} = 1$). The ratio depends on the value of the parameter u. For $u < u_m$ the lower steady state is dominant whereas for $u > u_m$, the higher one becomes dominant. This is expected for a large system when observations are made on a time scale far longer than the kinetic processes occurring in the system. Otherwise, the hysteresis will be observed.

References

1. M. Schell, K. Kundu and J. Ross, *Proc. Natl. Acad. Sci.*

USA, **84**, 424 (1987).

2. Y. Termonia and J. Ross, *Proc. Natl. Acad. Sci. USA,* **78**, 3563 (1987); **79**, 2878 (1982).
3. J. J. Tyson and H. G. Othmer, *Prog. Theor. Biol.,* **5**, 1 (1978).
4. C. L. Creel and J. Ross, *J. Chem. Phys.,* **65**, 3779 (1976).
5. J. Keizer, *Proc. Natl. Acad. Sci. USA,* **75**, 424 (1978).
7. G. Yagil and E. Yagil, *Biochem. J.,* **11**, 11 (1971).
8. I. Procaccia and J. Ross, *J. Chem. Phys.,* **67**, 5565 (1977).
9. J. Keizer, *J. Chem. Phys.,* **65**, 4431 (1976).
10. C. J. Kim, D. J. Lee, K. J. Shin, J. M. Lee, S. B. Ko and I. C. Jeon, *Bull. Korean. Chem. Soc.,* **10**, 452 (1989).
11. A. Nitzan, P. Ortoleva, J. Deutch and J. Ross, *J. Chem. Phys.,* **61**, 1056 (1974).
12. J. Hervagault, M. C. Duban, J. P. Kernevez and D. Thomas, *Proc. Natl. Acad. Sci. USA,* **80**, 5455 (1987).

Inter- and Intra-granular Critical Current in $Bi_{1.4}Pb_{0.6}Sr_2Ca_2Cu_{3.6}O_x$ Superconducting Oxide

Jin-Ho Choy[†] and **Seung-Joo Kim**[*]

[*]*Department of Chemistry,* [†]*Research Institute of Molecular Science, College of Natural Sciences, Seoul National University, Seoul 151 - 742*

J.C. Park, K. Frohlich, P. Dordor, and J.C. Grenier

Laboratoire de Chimie du Solide du CNRS, Université de Bordeaux I, 33405 Talence Cedex, France.

A.c. susceptibility for $Bi_{1.4}Pb_{0.6}Sr_2Ca_2Cu_{3.6}O_x$ superconductor is measured as a function of temperature at different value of a.c. magnetic field amplitude. Two transition steps are attributed to the intergranular and intragranular properties. Based on Bean's critical state model, intergranular critical current density, J_c^{gb} (11 A/cm^2 at 77 K) and intragranular critical current density, J_c^g (7×10^3 A/cm^2 at 100 K) are estimated. The low values of J_c^{gb} and J_c^g reflect a poor nature of coupling between grains and the low pinning force density of intragrain in $Bi_{1.4}Pb_{0.6}Sr_2Ca_2Cu_{3.6}O_x$ superconductor.

Introduction

Recently, a new superconducting Bi-Sr-Ca-Cu-O system with high critical temperature was discovered.[1] The Bi-Sr-Ca-Cu-O system mainly contains two superconducting phases, $Bi_2Sr_2Ca_2Cu_3O_x$ (2223 phase) and $Bi_2Sr_2Ca_1Cu_2O_x$ (2212 phase) with T_c of 110 K and 80 K, respectively. Partial substitution of Bi by Pb was found to increase the volume fraction of the 2223 phase.[2] Furthermore, it has been reported that addition of Pb prevents stacking faults of the layer structure and promotes crystallization of the 2223 phase.[3]

In this work, the magnetic and current transport properties of the Bi-Pb-Sr-Ca-Cu-O system are studied by a.c. magnetic susceptibility ($X = X' - iX''$) measurements. The changes of the real part signal X' and the imaginary part signal X'' with respect to the temperature are caused by induced shielding current and hysteresis losses, respectively,[4,5] which are related to the critical current density, J_c. The

purpose of this study is to estimate the critical current density of $Bi_{1.4}Pb_{0.6}Sr_2Ca_2Cu_{3.6}O_x$ superconductor and to describe the nature of coupling between grains and the intrinsic superconducting property.

Experimental

The 2223 phase was prepared by solid state reactions of a mixture of Bi_2O_3, $PbCO_3$, $SrCO_3$, $CaCO_3$ and CuO with the nominal composition of $Bi_{1.4}Pb_{0.6}Sr_2Ca_2Cu_{3.6}O_x$. The mixed powder was pressed into pellets, and then calcined at 810 °C for 24 hr in air. The resulting pellet was reground, pelletized and finally sintered at 855 °C for 160 hr in air then slowly cooled down to room temperature.

The product was characterized by powder X-ray diffraction with Ni-filtered Cu-K$_\alpha$ radiation. The temperature dependence of electrical resistivity was measured with a conventional four probe method. The microstructure was observed by scanning electron microscope (SEM).
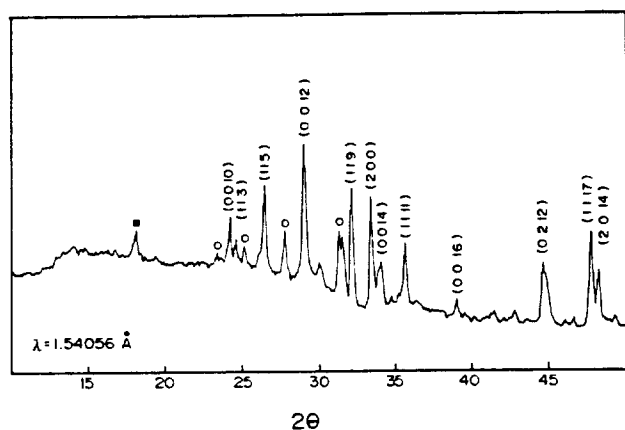
Figure 1. X-ray powder diffraction patterns of $Bi_{1.4}Pb_{0.6}Sr_2Ca_2$-$Cu_{3.6}O_x$. The peaks denoted by (hkl), $\bigcirc$ and $\blacksquare$ respectively correspond to the 2223 phase, the 2212 phase and the insulating one.
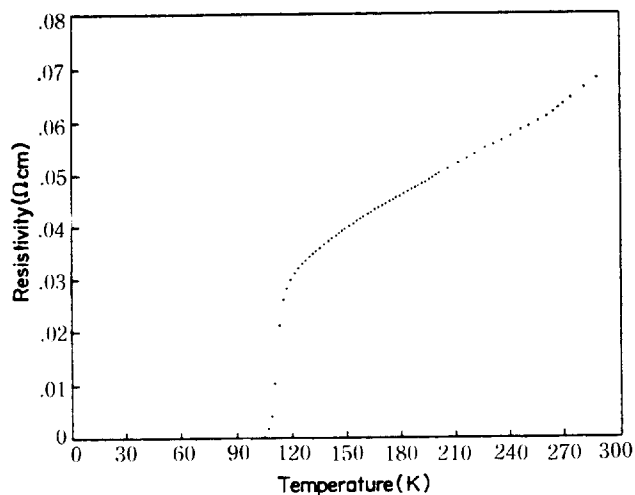

Figure 3. Scanning electron macroscopic image of the sample.

Figure 2. Temperature dependence of the electrical resistivity for $Bi_{1.4}Pb_{0.6}Sr_2Ca_2Cu_{3.6}O_x$.

A.c. susceptibility was measured as the function of temprature with a computer controlled mutual inductance bridge (ATNE PMSO2). The two phase sensitive detectors simultaneously supply the signal in phase (χ') and out phase (χ'') informations. The sample was parallelepiped shape (1.85 × 1.85 × 7.0 mm³) and placed inside a pick-up coil coaxial with primary coil. Before introduction of the sample, the signal of the secondary coil could be compensated by series matched counterwound coil. The primary coil was fed with an a.c. current (frequency = 123 Hz). Both primary and secondary coils were kept at liquid nitrogen temperature, while the temperature of the sample was swept between 78 K and 110 K. The χ' signal of the pick-up coil was calibrated against a ferrite sphere

Results and Discussion

Figure 1 shows the X-ray diffraction patterns for $Bi_{1.4}Pb_{0.6}$-$Sr_2Ca_2Cu_{3.6}O_x$. The indexed peaks agree with those of the 2223 phase, while the peaks indicated by open circles and solid square are consistent with those of 2212 phase and Ca_2PbO_4 impurities, respectively. It is clear that 2223 phase
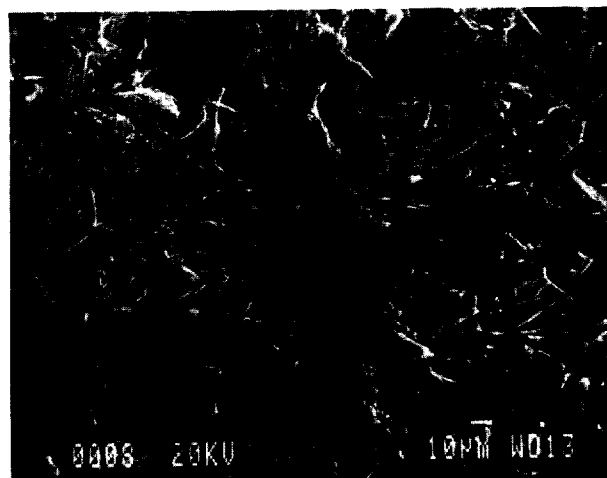
is dominant in this sample. The calculated lattice parameters are $a = 5.394$ Å and $c = 37.062$ Å.

The electrical resistivity vs. temperature indicates a superconducting transition at 113 K, with the zero resistivity temperature of about 103 K (Figure 2).

The SEM image of the sample shows plate like grains distributed without any preferential orientation (Figure 3). The average dimension is approximately 2 μm thick and 10-20 μm wide.

The real and imaginary parts of the susceptibiliy of $Bi_{1.4}Pb_{0.6}Sr_2Ca_2Cu_{3.6}O_x$ are plotted in Figure 4 (a) as a function of temperature for various a.c. field amplitudes. The curves show a characteristic two-step transition for χ' and two corresponding peaks for χ'' as previously observed for other superconducting oxides exhibiting an average grain size of about 10 μm.[6-8]

The transition from normal to superconducting state begins at 107 K irrespectively to the applied field amplitude. Just below the critical temperature, χ' at first steeply decreases down to -0.2 and χ'' increases to reach a maximum at a temperature ($T = T_m^g$), then decreases with the temperature. T_m^g is insensitive to the applied magnetic field strength as shown in Figure 4(b). Below 104 K, χ' gently decreases down to a constant value at least for the lowest fields, whereas χ'' exhibits large peak with maximum occurring at T_m^{gb}. However, T_m^{gb} is strongly dependent on the magnetic field amplitude.

Such a behavior has been interpreted in terms of superconducting grains presumably coupled by weak links behaving like Josephson junctions.[9,10]

The highest transition temperature is associated with intragranular properties. With decreasing temperature $T_m^g < T < T_c$, the grains become superconducting and intragranular supercurrent flows in leading to an enhanced screening, i.e. lower χ' and higher χ''. χ'' increases until temperature reaches T_m^g, at which the a.c. magnetic field just vanishes in the center of the grains. Below T_m^g, χ'' decreases because the field penetrates no longer the whole grain volume and the volume shrinks, in which hysteresis losses occur.

The lowest transition temperature reflects the intergranular properties of the sample. As the Josephson coupling energy E_J exceeds thermal activation energy kT, the
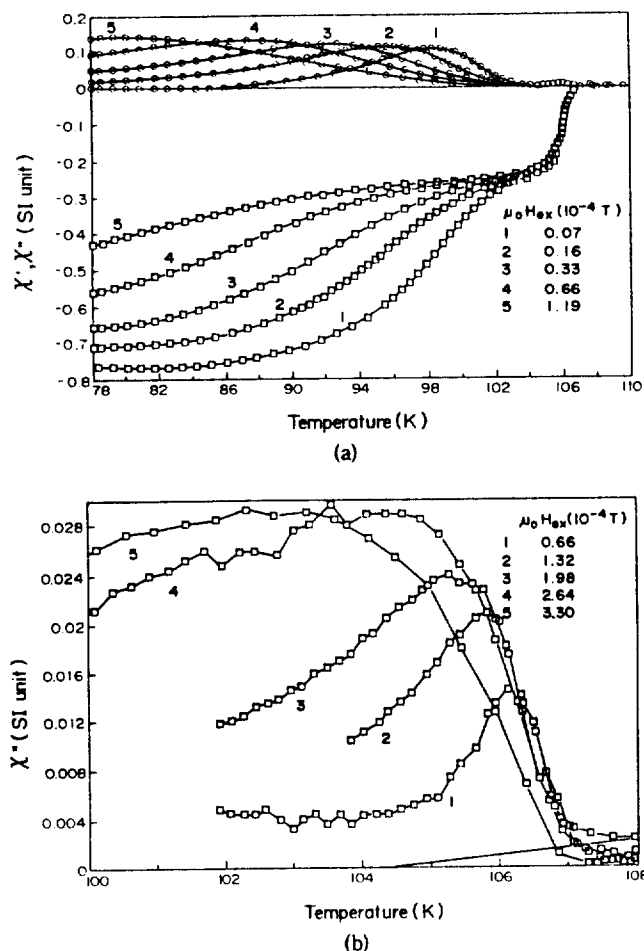
Figure 4. (a) Temperature dependence of a.c. magnetic susceptibility of $Bi_{1.4}Pb_{0.6}Sr_2Ca_2Cu_{3.6}O_x$ at various external magnetic field amplitudes. (b) Imaginary part of a.c. magnetic susceptibility in the temperature range of 100 K–108 K.

shielding current starts to flow through intergranular region, χ' decreases and χ'' increases. At T_m^{gb}, the shielding current begins to screen the center of the bulk sample and the value of χ'' reaches to a maximum.

The experimental amplitudes of χ'' are smaller than the theoretical value (0.212 for long cylindrical sample[11]) as shown in Figure 4. This deviation is due to: (i) the small volume fraction of superconducting material in sample. Even at 78 K, no perfect screening is appeared, (*i.e.* the value of χ' is –0.8 for $\mu_o H_{ex} = 0.07 \times 10^{-4}$ *T*.) which could be connected with the rather low density of the sample and/or with the existence of impurity phases. (ii) the superconducting volume reduction associated with London penetration length λ. (This effect is considerable in the case of intragranular energy losses because λ is comparable to grain size R_g.)[12]

According to the previous works[13-15] showed that it was possible to estimate the current density (J_c) at a given temperature from the position of χ'' peaks on the basis of Bean's critical state model.[15] In this model, the current flowing in the superconductor is taken to be equal to the critical current or to zero and the value of the critical current is independent of the magnetic field. Therefore, the flux density profiles in the sample show a linear decay with a slope ($=J_c$). When χ'' is maximum, the relation between magnetic field
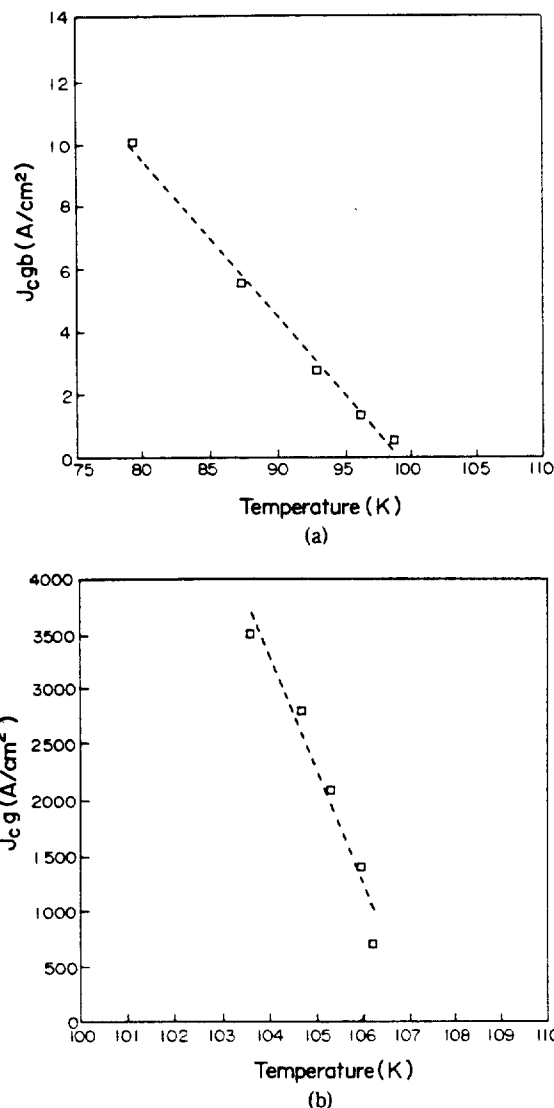

Figure 5. Temperature dependence of (a) intergranular critical current density (J_c^{gb}) and (b) intragranular critical current density (J_c^g).

and critical current density for cylindrical shaped sample is expressed as

$$H_s = J_c R, \qquad (1)$$

where R is the radius of cylinder, H_s is the a.c. magnetic field at the surface of the sample estimated from the following relation.[17]

$$H_s = H_{ex}/(1-D). \qquad (2)$$

H_{ex} is the applied magnetic field and D the demagnetization factor. In order to evaluate the intergranular critical current density J_c^{gb}, we regard the parallelepiped shaped sample as a cylinder with an equivalent cross section and a demagnetization factor of the sample ($D \simeq 0.1$[18]).

Figure 5 (a) represents, J_c^{gb} of $Bi_{1.4}Pb_{0.6}Sr_2Ca_2Cu_{3.6}O_x$ sample at peak maximum temperature T_m^{gb}. The values are much smaller than those measured for other superconducting oxide like $YBa_2Cu_3O_{7-\delta}$ (200–1000 A/cm²). J_c^{gb} at 77 K is only 11 A/cm² for our samples. Such a low critical current density can be ascribed to weak links between grains.
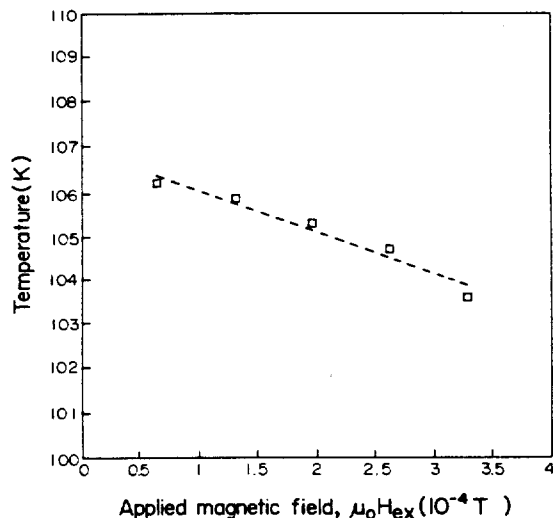
Figure 6. Field dependence of T_m^g of $Bi_{1.4}Pb_{0.6}Sr_2Ca_2Cu_{3.6}O_x$.

Replacing R by the average grain radius (R_g) in equation (1), intragranular critical current density J_c^g can be roughly estimated. From the SEM image (Figure 3), R_g is approximated to 5–10 μm, nevertheless such an estimation may introduce a systematic error in J_c determination because the grain shape is anisotropic. Figure 5(b) shows the values of J_c at T_m^x. By a linear extrapolation over a small temperature range, J_c^g can be deduced (about 7×10^3 A/cm^2) at 100 K, disregarding the contribution of demagnetization factor of grains. The low value is related to weak pinning force which is measurable from a.c. susceptibility on the basis of Müller's work.[19] Considering magnetic independent pinning force density α_v for intragranular flux vortices, the relation of T_m^g's and applied magnetic field amplitudes are obtained as follows

$$T_m^g = T_c - T_c \left(\mu_0/8R_g\alpha_g(0)\right)^{1/2} H_{ex}$$

From the slope of T_m^x versus H_{ex} in Figure 6, $\alpha_g(0)$ is extracted to be 1.6×10^6 TAm^{-2}. The value is one order lower than for $YBa_2Cu_3O_{7-\delta}$ (3×10^7 TAm^{-2}).[19] The reason for the lower value of $\alpha_g(0)$ for $Bi_{1.4}Pb_{0.6}Sr_2Ca_2Cu_{3.6}O_x$ is the lack of pinning center such as twin boundaris for $YBa_2Cu_3O_{7-\delta}$.[20-21]

In conclusion, the low current carrying capability for polycrystalline $Bi_{1.4}Pb_{0.6}Sr_2Ca_2Cu_{3.6}O_x$ is attributed to the weak couplings between superconducting grains and to the small number of pinning center within grain.

Acknowledgement. This research is supported by the grant from the Korean Ministry of Science and Technology.

Reference

1. H. Maeda, Y. Tanaka, M. Fukutomi, and T. Asano, *Jpn. J. Appl. Phys.*, **27**, L209 (1988).
2. U. Endo, S. Koyma and T. Kawai, *Jpn. J. Appl. Phys.*, **27**, L1476 (1988).
3. M. Mizuno, H. Endo, J. Tsuchiya, N. Kijima, A. Sumiyama, and Y. Oguri, *Jpn. J. Appl. Phys.*, **27**, L1225 (1988).
4. E. Maxwell and M. Strongin, *Phys. Rev. Lett.*, **10**, 212 (1963).
5. T. Ishida and H. Mazaki, *J. Appl. Phys.*, **52**, 6798 (1981).
6. H. Mazaki, M. TaKano, R. Kanno and Y. Takeda, *Jpn. J. Appl. Phys.*, **26**, L780 (1987).
7. H. Mazaki, M. TaKano, Y. Ikeda, Y. Bando, R. Kanno, Y. Takeda, and O. Yammamoto, *Jpn. J. Appl. Phys.*, **26**, L1749 (1987).
8. H. Küpfer, S. M. Green, C. Jiang, YuMei, H. L. Luo, R. Meier–Hirmer, and C. Politicis, *Z. Phys. B – Condensed Matter*, **71**, 63 (1988).
9. R. B. Goldfarb, A. F. Clark, A. I. Braginski, and A. J. Panson, *Cryogenics*, **27**, 475 (1987).
10. D. X. Chen, J. Nogues and K. V. Rao, *Cryogenics*, **29**, 800 (1989).
11. J. R. Clem, *Physica C.*, **153-155**, 50 (1988).
12. H. Küpfer, I. Apfelstedt, R. Flükinger, C. Keller, R. Meier–Hirmer, B. Runtsch, A. Turowski, U. Wiech, and T. Wolf, *Cryogenics*, **28**, 650 (1988).
13. F. Gömöry and P. Lobotka, *Solid State Commun.*, **66**, 645 (1988).
14. S. D. Murphy, K. Renouard, R. Crittenden, and S. M. Bhagat, *Solid State Commun.*, **69**, 367 (1989).
15. V. Calzona, M. R. Cimberle, C. Ferdeghini, M. Putti, and A. S. Siri, *Physica C*, **157**, 425 (1989).
16. C. P. Bean, *Rev. Mod. Phys.*, **36**, 31 (1964).
17. L. D. Landau and E. M. Lifshitz, "Electrodynamics of continuous media", p. 170, Pergamon Press.
18. American Institute of Physics Handbook, 3rd Ed. p. 5-247.
19. K. H. Müller, *Physica C.*, **159**, 717 (1989).
20. Y. Yeshurun, A. P. Malozemoff, T. K. Worthington, R. M. Yandrofski, L. Krusin–Elbaum, F. H. Holtzberg, T. R. Dinger, and G. V. Chandrashekhar, *Cryogenics*, **29**, 258 (1989).
21. M. M. Fang, V. G. Kogen, D. K. Finnemore, J. R. Clem, L. S. Chunbley, and D. E. Farrell, *Phys. Rev. B.*, **37**, 2334 (1988).